UNIVERSITY OF PITTSBURGH

ORTHOPAEDIC ROBOTICS LABORATORY

2022 SUMMER UNDERGRADUATE ABSTRACT BOOKLET

FOREWARD

The Orthopaedic Robotics Laboratory is the University of Pittsburgh's newly formed collaborative effort between the Department of Bioengineering and Department of Orthopaedic Surgery. The mission of the ORL is the prevention of degenerative joint diseases by improving diagnostic, repair, and rehabilitation procedures for musculoskeletal injuries using state-of-the-art robotic technology. The ORL would like to commend the work of the undergraduate students during the summer of 2022. Students made significant impacts in the study of shoulder and elbow degenerative joint diseases. The work of our students, with the help of our mentors, contributes greatly to world of Orthopaedic Research and to all patients who benefit.

OUR TEAM

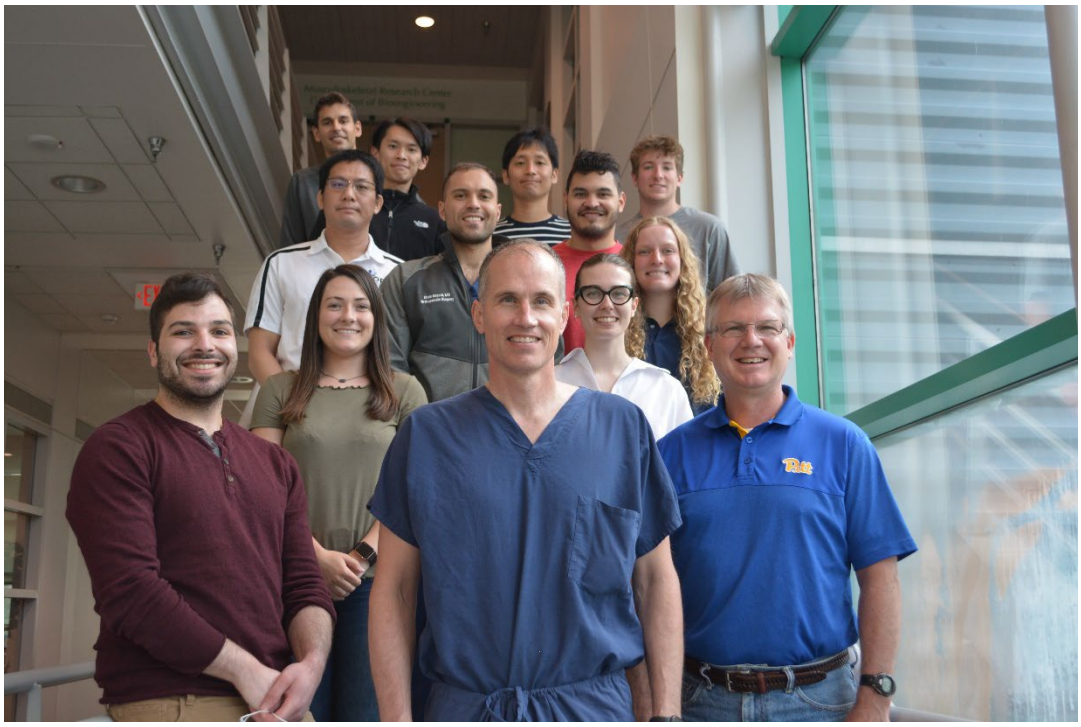

Benjamin Newell
Class of 2023
Bioengineering
University of Pittsburgh

Abigail Book
Class of 2023
Bioengineering
University of Pittsburgh

TABLE OF CONTENTS

Surface Area of the Glenohumeral Capsule following Multiple Anterior Dislocations in High Non-Recoverable Strain Regions

Abigail Book[1]; Keishi Takaba[2]; Sene Polamalu[1]; Ehab Nazzal[2]; Satoshi Takeuchi[2]; Volker Musahl[1,2]; Albert Lin[2]; Richard E. Debski[1,2]

[1]Department of Bioengineering & [2]Department of Orthopaedic Surgery, University of Pittsburgh, Pittsburgh, PA

INTRODUCTION: The glenohumeral joint is the most commonly dislocated joint, resulting in greater than 80% anterior dislocations [1]. Arthroscopic Bankart repair is the most common surgical procedure to treat anterior dislocations, however, the dislocation reoccurrence rate is up to 22% [2]. The glenohumeral capsule experiences non-recoverable stain after dislocation, in addition to Bankart lesions [3]. Capsular plication can be done in addition to the Bankart repair to help decrease the reoccurrence rate of dislocations and shoulder instability. However, the procedure is based on the surgeon's experience, and with minimal information on the optimal direction of suture placement. Non-recoverable strain can be a measure of capsular injury, but the relationship between strain and surface area is unknown following anterior dislocations. Surface area is the quantity that is measurable in human subjects. The first objective of this study is to verify multiple algorithms to calculate surface area of the shoulder capsule using a balloon model. The second objective of this study is to determine the surface area of the glenohumeral capsule in regions that were plicated based on high non-recoverable strain during repair procedures in a cadaveric model.

BALLOON TESTS: A balloon was blown up to a circumference of 200 mm, mimicking an intact shoulder capsule. A 4 x 4 grid of markers were drawn on the surface of the balloon. The marker locations were recorded and tracked using a DMAS 7 Motion Capture System (Spica Technology Corporation, Haiku, HI). The distances between the centroids of the markers were also measured using calipers. The balloon was then blown up to a circumference of 210 mm, mimicking the shoulder capsule with 5% strain. The marker locations were again recorded and tracked, as well as the distances between the centroids of the markers. The surface area of both conditions was calculated using ABAQUS (ABAQUS/Viewer Student Edition 2021; Simulia, Providence RI) and MATLAB (MATLAB & Simulink R2020b; MathWorks, MA, USA). The 2D area was calculated from measured distances using MATLAB. The non-recoverable strain was calculated using ABAQUS. This procedure of blowing up the balloon to capsular size and calculating surface area and strain was repeated a second time, in addition to increasing the circumference by 10 mm each time, mimicking increasing strain (5%, 10%, 15%, 20%, and 25%).

RESULTS: ABAQUS resulted in a 14 mm^2 difference between the 'intact' and '+5%' states. MATLAB also resulted in a 14 mm^2 difference between the 'intact' and '+5%' states. Using calipers for a 2D approximation, the difference between the 'intact' and '+5%' states was 10 mm^2. Using ABAQUS, the non-recoverable strain was averaged to be 6.0%. As circumference increased by 10mm, surface area also increased, as well as resulting strain (**Table 1**).

	SA Calculated [mm^2]	SA Increase (%)	Average Strain (%)
'Intact'	271		
'+5%'	283	4.4	4.9
'+10%'	299	10.5	11.0
'+15%'	308	13.7	14.6
'+20%'	329	21.5	18.1
'+25%'	350	29.2	23.1

Table 1: Surface Area changes from intact to the increased state, in mm^2 and percent difference. Average strain calculated for each state.

DISCUSSION: Surface area was similar between ABAQUS and MATLAB, and comparable to the 2D area found using calipers. This verified that the algorithms being used, ABAQUS and MATLAB, can correctly output the surface area of the shoulder capsule. Strain was also within repeatability of 3% of the desired strain [1]. Also, as strain increased, the surface area increased linearly. High non-recoverable strain should result in increased surface area.

CADAVERIC TESTS: Eight fresh-frozen cadaveric shoulders were dissected, leaving only the scapula, humerus, glenohumeral capsule, and coracoacromial and coracohumeral ligaments. A 7 x 11 grid of strain markers are fixed onto the capsule. The shoulders are mounted onto the 6 degree of freedom robotic testing system and 77 markers on the glenohumeral capsule are tracked. The position of the shoulder with

minimal pressure inserted that allows for the least amount of marker movement was used as the reference state. The glenohumeral joint was then dislocated anteriorly 5 times and the joint was returned to the reference state for marker locations to be tracked again. The coordinates from marker tracking are used to determine the non-recoverable strain distribution using ABAQUS. The 7 x 11 grid can be broken into 8 subregions, the anterior band of IGHL, the anterior axillary pouch, the posterior axillary pouch, and the posterior band of IGHL, each having glenoid and humeral regions. Quantification of strain values for each subregion of the capsule was collected, and those with higher than the average value were plicated. Surface area of those plicated subregions was found using MATLAB and ABAQUS for both the intact and after 5 dislocations states.

RESULTS: Surface area of plicated subregions of the glenohumeral capsule results in some increases and some decreases when comparing the intact and after 5 dislocation states. Surface area is compared between the intact state and after 5 dislocations. (**Table 2**). Out of 20 regions that were plicated, 7 decreased in surface area and 13 increased. Five decreases occurred in the glenoid region, while two occurred in the humeral regions. When comparing anterior versus posterior decreases, five occurred in the anteriorly while two occurred posteriorly. When comparing where increases occurred, eight were on the glenoid side while five were on the humeral side; five occurred anteriorly and eight occurred posteriorly.

Test	Subregions	Strain (%)	SA change [mm^2]
1	ABG	8.3	-1.2
	PAPG	6.2	5.4
	PBH	11.9	10.8
3	ABH	5.9	0.1
	AAPG	5.4	-12.3
	PBG	5.4	6.1
6	ABG	7.1	-1.1
	AAPG	5.0	1.6
	ABH	5.1	3.6
7	PBG	3.8	1.2
	PAPG	4.5	2.1
	PBH	3.9	-8.0
	PAPH	7.3	10.6
9	PBG	4.6	2.6
	AAPG	5.4	3.9
	ABG	5.3	-0.4
	AAPH	6.9	0.5
10	PBG	6.2	-5.5
	PAPG	9.8	8.1
	ABH	6.2	-3.4

Table 2: Surface area of subregions that were plicated based on high non-recoverable strain. Anterior band of IGHL (AB), anterior axillary pouch (AAP), posterior axillary pouch (PAP), posterior band of IGHL (PB), glenoid (G), humerus (H).

DISCUSSION: When finding surface area of the glenohumeral capsule in high non-recoverable strain areas, calculated surface area did not always result in an increase. In cases where the surface area decreased, human error could have occurred when inserting minimal pressure into the capsule or the distribution of pressure was not even across the capsule. During a supplemental analysis, different angles of the pressure nozzle and the depth of nozzle insertion had an effect on surface area calculations. This could lead to wrinkles and/or folds within the capsule allowing for incorrect calculations. Future studies will include more cadaver tests and come up with a relationship between surface area changes and the amount of non-recoverable strain. Within those future studies, clinicians should keep a constant angle and depth when inserting the pressure nozzle.

SIGNIFICANCE: The findings of the balloon test showed that ABAQUS and MATLAB could accurately process data, and as strain increased, surface area increased linearly. However, it is recommended to maintain a constant pressure nozzle angle and insertion depth during cadaveric tests, and to document clearly that angle and depth. In the future, these findings can be used to help assess surface area data from MR arthrograms to link cadaveric and human subject data. In areas where an increase in surface area occurs, high non-recoverable strain probably occurs, and surgeons should plicate these regions during repair procedures.

ACKNOWLEDGEMENTS: Support from the University of Pittsburgh Swanson School of Engineering, Department of Bioengineering, and Department of Orthopaedic Surgery is gratefully acknowledged.

REFERENCES:

[1] Moore JOR 2008
[2] Bessiere CORR 2014
[3] Malicky JBE 2001

Identifying the Inferior Glenohumeral Ligament in 3D MRI Reconstructions

Benjamin W. Newell[1,3], Zachary J. Herman MD[1,2], Ehab M. Nazzal MD[1,2], Keishi Takaba MD[1,2], Volker Musahl MD[1,2,3], Chan Hong Moon[4], Albert Lin MD[1,2], Richard E. Debski PhD[1,2,3]

1. Orthopaedic Robotics Laboratory, University of Pittsburgh, Pittsburgh, PA
2. Department of Orthopedic Surgery, University of Pittsburgh, Pittsburgh, PA
3. Department of Bioengineering, University of Pittsburgh, Pittsburgh, PA
4. Department of Radiology, University of Pittsburgh, Pittsburgh, PA

INTRODUCTION: The glenohumeral joint is the most dislocated joint in the human body[1]. After repeated dislocations, the capsule, particularly the inferior glenohumeral ligament (IGHL), suffers non-recoverable strain[2]. The IGHL is comprised of 3 regions, the anterior band, posterior band, and axillary pouch, but can be observed as a single sheet of tissue with anterior and posterior thickenings[3,4]. Clinically, dislocations result in glenohumeral joint instability requiring surgical intervention in the form of plication. Currently, plicated locations are subjectively determined by the operating surgeon. Ideally, identifying the individual regions of the IGHL that suffer non-recoverable strain after dislocation would give orthopaedic surgeons the information necessary to perform subject specific plications, which may improve treatment outcomes. Previous cadaveric studies have placed markers on the IGHL and determined non-recoverable strain in regions of the IGHL after simulated dislocation[2]. However, a similar methodology cannot be utilized in patients clinically as the dislocation has already occurred and markers cannot be placed in vivo. This methodology would require accurate and repeatable identification of the IGHL on MRI reconstructions to quantify surface area. Thus, the goal of the project was to determine the intra- and inter-observer repeatability of identifying the four corners of the IGHL on a 3D shoulder model created from an MRI of a cadaveric shoulder to aid in identification of injured regions of the capsule.

METHODS: In order to produce markers that could be used on a motion tracking system and seen on MRI, a novel method was created by soaking canola seeds in a gadolinium solution. Four markers were fixed on the corners of the IGHL in a cadaveric shoulder. Previous work in the laboratory has shown the ability to measure distances between two markers on 3D reconstructions with an accuracy of ± 0.6 mm compared to a gold standard. The markers were placed 5 mm from the insertion sites in the medial or lateral direction, respectively, of the anterior and posterior bands of the glenoid and humerus. The shoulder was mounted onto a custom fixture in 90 degrees of abduction and external rotation (ABER) and imaged via MRI using 3T (Siemens, mMR Biograph) and flexible 4ch coil (target volume fully wrapped by the coil), TR/TE 15/2.85 ms, isotropic voxel 400 um. The humerus, glenoid, IGHL, and markers were segmented to create a 3D model of the glenohumeral joint and IGHL in MIMICs (version 23.0). A protocol to identify and mark the corners of the IGHL on the 3D model of the shoulder was given to three observers with differing anatomic knowledge, and a custom MATLAB code was used to measure the 3D distance from observer-placed markers to the canola seed marker location based on MRI segmentation. All observers were blinded to the true location of the canola seed markers. Each observer repeated the protocol three times. Average distance from the estimated to actual marker was used to identify accuracy, while standard deviations were used to determine intra- and inter-observer repeatability. A Welch test with Games-Howell post hoc analysis were used to compare marker placement accuracy, and an F-test with Tukey post hoc analysis were used to compare marker placement repeatability.

RESULTS: The novel canola seed markers were seen clearly in the MRI and easily reconstructed. The anatomy of the joint included the collar-like insertion of the IGHL around the glenoid and V-shaped

insertion on the humerus. The dashed lines in the figure show the range of error in marker placement for each of the markers. Observer 1 demonstrated an intra-observer repeatability of 0.4 mm for the glenoid insertion of the anterior band (GAB), 0.2 mm glenoid insertion of the posterior band (GPB), 2.0 mm for the humeral insertion of the anterior band (HAB), and 0.1 mm for the humeral insertion of the posterior band (HPB). For all observers, placement of the GAB marker was most accurate, at 3.3 ± 0.7 mm ($p < 0.001$ for all pairwise comparisons), and the HPB was the least repeatable ($p < 0.01$ for all pairwise comparisons).

DISCUSSION: The gadolinium-soaked markers were successfully visualized on MRI, and thus, this methodology can be utilized in subsequent studies. The proposed method for identifying capsular borders was accurate to 6.9 mm and repeatable to 2.3 mm. Accuracy was affected by the fact that observers picked 3D marker locations on the surface of the capsule, while experimentally glue was used to place canola seeds, which elevated the markers from the surface of the capsule. The points with the smallest average distance (GAB, GPB) may be the result of well-defined insertions on the glenoid rim, while markers that were more inaccurate (HAB, HPB) and less repeatable (HPB) may be attributed to the indistinct, V-shaped insertion of the IGHL on the humerus. Previously, anatomical landmarks on the femur of 3D printed knees were located with an error ranging from 3.9-11.1 mm after a teaching session[5]. These results are on the same order of magnitude as our findings, providing further validation of our results. The long-term goal of this work is to determine the differences in injured and contralateral shoulders with respect to the geometry of the glenohumeral capsule. Future investigation is necessary to determine how alterations in marker placement accuracy affect capsular geometry.

CLINICAL RELEVANCE: The ability to repeatably identify the IGHL on 3D reconstructed models will allow division of the capsule into smaller regions to determine the locations where the capsule may be injured. Once the regions are determined, injured shoulders can be compared to contralateral shoulders in vivo to provide surgeons with information to guide subject specific plications.

REFERENCES: 1. Nabain et al. ABJS, 2017 2. Yoshida et al. JOR, 2020 3. Moore et al. Ann Biomed Eng, 2009 4. O'Brien et al. AJSM, 1990 5. Laverdiere et al. OJSM, 2020

Table 1. Average distance between estimated marker and nearest edge of canola seed marker for each observer. Glenoid insertions of anterior and posterior bands indicated by GAB and GPB. Humeral insertions of anterior band and posterior band indicated by HAB and HPB.

Observer	GAB (mm)	GPB (mm)	HAB (mm)	HPB (mm)
1	2.7	3.8	7.4	7.9
2	3.0	4.1	6.2	4.6
3	4.1	5.5	7.1	3.5
AVG	3.3	4.5	6.9	5.3
SD	0.7	0.9	0.6	2.3

Figure 1. 3D reconstruction of the glenoid (yellow), humerus (green), IGHL (blue), and 4 canola seed markers (black). Dashed lines represent error in marker placement. Markers enlarged for visualization.

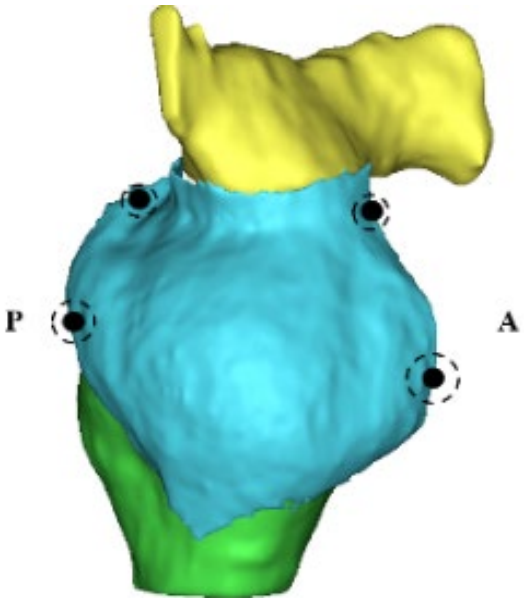

Behavior of Intramedullary Screw Fixation in Humeri and Ulnae for Total Elbow Arthroplasty

Benjamin W. Newell[1,3], Ehab M. Nazzal[1,2], Luke T. Mattar[1,3], Robert A. Kaufmann[1,2], Richard E. Debski[1,2,3]

1. Orthopaedic Robotics Laboratory, University of Pittsburgh, Pittsburgh, PA
2. Department of Orthopedic Surgery, University of Pittsburgh, Pittsburgh, PA
3. Department of Bioengineering, University of Pittsburgh, Pittsburgh, PA

INTRODUCTION: Non-reconstructable distal humerus fractures and elbow dysfunction secondary to rheumatoid arthritis, degenerative osteoarthritis, or post-traumatic osteoarthritis can be treated with total elbow arthroplasty (TEA)[1-3]. Currently TEA has an overall complication rate of 25% and an 11-year survival rate that is less than 80% and is much lower than that of hip and knee arthroplasty which have a 96% 10-year survival rate[3-5]. Loosening is the most common cause of failure effecting TEA[6]. Currently implants utilize bone cement to hold the stems in place. Bone cement has been used since the 1950s and has negative effects including thermal osteonecrosis which is due to the sudden increase in heat that damages the surrounding bone causing loss in ability to heal and grow[7,8]. Additionally, cement is difficult to remove making revision surgery more complicated and time consuming. Due to the complications associated with cement implant fixation, the feasibility of intramedullary screw fixation needs to be assessed for use in TEA. The objective of this study is to determine structural properties of the bone-screw interface for TEA and assess the effectiveness of this method of implantation based on data in the literature.

METHODS: Seven fresh frozen upper extremity cadavers (age: 61 ± 14 years) were prepared by removing all soft tissue from the humeri and ulnae and then drilled at the end proximal to the elbow with custom drill bits, increasing in diameter until chatter was felt from reaching cortical bone. Once chatter was experienced, the specimens were hand tapped with the thread size corresponding to the drill bit and then custom-made titanium screws were screwed into the intramedullary canals until seated. The specimens were then potted in an epoxy putty and mounted to the base of a uniaxial materials testing machine (Instron, Model 5695) in a custom fixture. The screw head was aligned with the testing machine to ensure that no bending moments were applied and then preloaded to remove slack before being preconditioned from 30-66 N for 10 cycles. Next, the specimen was loaded at a rate of 5mm/min until the load reached 3kN, the force that can be reached during strenuous isometric actions[9]. To ensure safety, the test was also terminated based on two criteria: 1) a decrease of 200N, or 2) extension beyond 70 mm. At the conclusion of each test, the specimen was inspected for evidence of pullout, loosening, or visible fractures. End-of-test elongation, load, energy absorbed, and stiffness were calculated. End-of-test load and elongation were defined as the elongation and load experienced by the structure at 3kN or failure. Stiffness of the linear region of the load-elongation curve was found by removing all points after end of test load, and then removing points from the start of the test until an $R^2>0.99$ was reached. Energy absorbed was determined by estimating the area under the curve from the beginning of the test until end of test using a trapezoidal Riemann sum.

RESULTS: 14 total tests were completed using 7 humeri and 7 ulnae. The load-elongation curves were mostly linear. (Figure 1 and 2) Some curves had small drops before continuing to end-of-test. The humeri had an end-of-test load of 2721.0 ± 738.4 N and an end-of-test elongation of 3.0 ± 0.9 mm. Ulnae reached 92% of the humeri end-of-test load at 2513.5 ± 677.6 N and 120% end-of-test elongation at 3.6 ± 0.6 mm. The stiffness of the humeri was 1076.9 ± 335.7 N/mm and the ulna had 73% of the stiffness at 789.6 ± 211.3 N/mm. Finally, the energy absorbed for the humeri was 3.6 ± 1.6 J which was 92% of the ulnae at 3.9 ± 1.1 J. One humerus and 3 ulnae failed before the end-of-test load of 3 kN. Of the four specimens that failed, two failures were due to screw pullout and two due to bone break.

DISCUSSION: The purpose of the study was to determine the structural properties of non-cemented intermedullary screw fixation for use in total elbow arthroplasty. The load-elongation curves were linear which is expected in bone. The small drops in the load-elongation curves of some of the specimens may be due to micro failures, however the screws were able to reseat and reach higher loads. The majority of specimens reached our end of test criteria with only 1 humerus and 3 ulnae failing before the predetermined 3 kN load. However, even those that failed reached end-of-test loads that prove to be adequate for fixation with an average end-of-test load of 1660.3 N, much higher than the current force needed for osteointegration[8]. Additionally, the typical allowed load post operatively is about 11 lbs in hand, which generates much less force in the elbow than what was found in this study[10].

CLINICAL RELEVANCE: The findings in this study show that IM screw fixation without the use of bone cement can withstand a force that is greater than the currently recommended post-operative load and is required for osteointegration in total elbow arthroplasty implantation.

REFERENCES: 1. Zhang et al. JHS, 2019 2. Samdanis et al. Shoulder & Elbow, 2019 3. Voloshin et al. JSES, 2011 4. Welsink et al. JBJS, 2017 5. Bayliss et al. Lancet, 2017 6. Prkic et al. AOTS, 2017 7. Whitehouse et al. eCM, 2014 8. Kaufmann et al. ASSH, 2019 9. Amis et al. J Biomechanics, 1980 10. S. Kumar, S. Mahanta IJO, 2013

Figure 1. Load vs. elongation curve of humeri. Tests that reached 3 kN shown in blue, failures shown in orange.

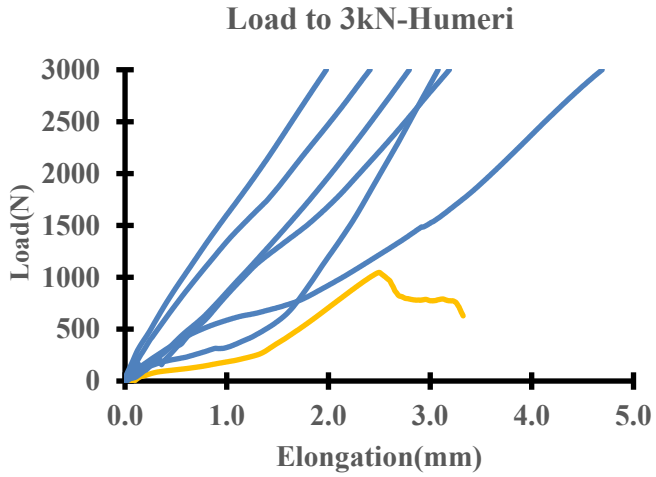

Figure 2. Load vs. elongation curve of ulnae. Tests that reached 3 kN shown in blue, failures shown in orange.